VARIABLE SPEED WECS USING SYNCHRONOUS GENERATORS CONNECTED TO ELECTRIC GRID THROUGH FREQUENCY CONVERTERS: MODELING AND SIMULATION

Geraldo Caixeta Guimarães, Adeon Cecilio Pinto, Bismarck Castillo Carvalho*, José Carlos de Oliveira, Adélio José de Moraes, Zélia da Silva Vitório**
Universidade Federal de Uberlândia, *Universidade Federal de Mato Grosso, **Furnas Centrais Elétricas
Av. João Naves de Ávila, 2121, Santa Mônica CEP 38400-902 - Uberlândia, MG, Brasil
adeon@eletrica,.ufu.br, bcc@ufmt.br, jcoliveira@ufu.br, gcaixeta@ufu.br, ajmoraes@ufu.br, zelia@furnas.com.br

***Abstract* – This paper deals with the time domain computer modeling for studying the behavior of WECS (Wind Energy Conversion Systems) connected to the utility grid system through frequency converters. Initially, it is presented the mathematical models for all parts of the variable speed wind system which uses, in the energy conversion process, a multipole synchronous generator. Because of the varying characteristic of the speed, this machine must employ an adequate converter to connect to the fixed frequency grid busbar. The behavior of the whole system is assessed through the monitored variables taken from the wind, going to the turbine-generator set, continuing to the converter and step-up transformer and ending at the grid busbar. Different conditions and variations imposed by the primary energy source (the wind) are taken into account together with their effects on WECS and electric grid coupling point. Besides that, this paper intends to fulfill an existing gap in the bibliography concerned to wind systems that employ synchronous generators which is the most predominant topology in the national market.**

***Keywords* – Modeling, synchronous generator, variable speed, wind energy.**

I. INTRODUCTION

Wind is one of the most important natural resources for the production of electricity. Due to its inexhaustible, worldwide potential, wind-produced electricity has been put forward as a possible way to substitute or to complement traditional fossil fuels. This substitution and/or complementation is becoming ever more necessary due to diminishing quantities and high prices of fossil fuels. During the past three decades, wind-turbine technology has been developed to such an extent that it is now becoming possible to use this technology to produce electricity at competitive prices [1]. Scientists predict that, by the year 2060, 50% of the total electric-power consumption in the world will be produced by wind turbines [2].

Wind systems with very advanced technological characteristics regarding driving speeds, electric generators and controllers have already been produced. The available literature on this subject deals mainly with asynchronous generators, with constant or variable speeds. There is, however, a great lack of literature regarding synchronous generators, which are widely used in Brazil. They are based on more recent technology. It is also important to mention that the only wind-turbine factory in Brazil produces machines based on this technology. Thus, this paper deals with the modeling and simulation of a variable speed wind energy conversion system (WECS) equipped with a synchronous machine powered by three wind-blades fixed to a horizontal shaft.

The WECS considered here uses a pitch control for the turbine blades, in accordance with the current world tendency [3], [4]. This control propitiates greater efficiency in energy extraction from the wind, especially for wind speed above rated. The pitch control philosophy is based on the independent rotation movement of the blades so as to reduce or increase the area under the action of the wind and, consequently, to maintain the output power approximately constant. Additionally, the only way to connect such type of wind system to the electric utility grid is using a frequency converter together with its designed control system.

Using such system, a comprehensive mathematical model is developed for the overall WECS, grid connection system and a time domain computational program is obtained. In addition to this, it must be emphasized that this work offers a complete computational tool that may attend the needs of the National Program of Alternative Energy Sources (PROINFA). This government program points out the exploration of 3,300 MW of power produced by alternative sources [5].

II. WIND ENERGY CONVERSION SYSTEM

The Wind Energy Conversion System (WECS) employed in this paper is composed of several subsystems, which begin with the wind representation and finish with the connection to the electric grid, as shown in Fig. 1.

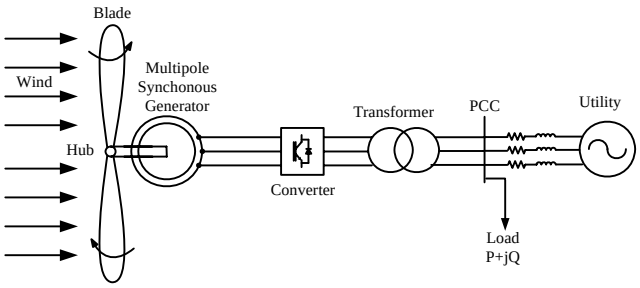

Fig. 1. Basic WECS used in the studies

Following, a summarized description of each WECS module is focused together with its mathematical representation.

A. Wind Representation

The wind signal representation is made through a formulation described in [6], that represents the sum of four components: the base wind speed (principal component); a gust; a speed ramp and a noise, according to (1).

$$V_{wind} = V_{base} + V_{gust} + V_{ramp} + V_{noise} \quad (1)$$

where:
V_{base} - wind base component;
V_{gust} - gust component;
V_{ramp} - ramp component;
V_{noise} - noise component.

B. Rotor Representation

The wind turbine rotor is responsible for the extraction of wind kinetic energy and for its transformation into rotational mechanical energy at rotor blades, transferring it to the electric generator shaft. The power developed by the three-blade rotor is determined by using a simplified model [3], given by (2). This equation shows that the mechanical power extracted from the wind is a function of cubic wind speed.

$$P_{mech} = \frac{1}{2}\rho A C_p(\lambda,\theta) V_{wind}^3 \quad (2)$$

where:
ρ - air density;
A - area swept by blades;
C_p - power or performance coefficient;
λ - blade speed ratio (tip speed ratio);
θ - blade pitch angle;
V_{wind} - wind speed.

The blade speed ratio is obtained by dividing the linear speed at the tip of blade (V_{blade}) by the wind speed (V_{wind}).

$$\lambda = \frac{V_{blade}}{V_{wind}} = \frac{\omega R}{V_{wind}} \quad (3$$

where:
R - blade radius;
ω - rotation speed.

The wind turbine model used in this study, as mentioned, permits the adjustment of the blade pitch angle (pitch control). Thus, the power coefficient (C_p) is a variable that depends on the blade speed ratio (λ), and the blade pitch angle (θ), as evidenced by (4).

$$C_p(\lambda,\theta) = 0{,}73\left(\frac{151}{\lambda_i} - 0{,}58\theta - 0{,}002\theta^{2{,}14} - 13{,}2\right)e^{\frac{-18{,}4}{\lambda_i}} \quad (4)$$

where:

$$\lambda_i = \frac{1}{\frac{1}{\lambda - 0{,}02\theta} - \frac{0{,}003}{\theta^3 + 1}} \quad (5)$$

C. Synchronous Generator Representation

One of the characteristics of the multipole generator used in this work is that it produces electricity efficiently when the rotating shaft spins at low speeds. Thus, it does not require a gearbox to increase the rotation, that is a permanent sources of mechanical problems and greatly increase maintenance and associated costs. This fact alone gives the multipole machine an enormous advantage over the induction generator used in other systems.

Fig. 2 shows a schematic representation of the six-winding synchronous machine in this work used to describe the general flux model [7], considering time domain techniques. The algebraic and differential equations give a detailed synchronous generator model which makes it possible to observe the subtransient phenomena that occur in the stator. This is very important in simulations that involve semiconductor electronic components, because the maximum transient current and voltage peaks are essential for the design of such devices.

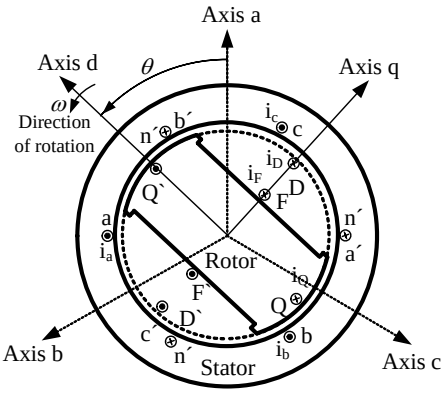

aa´, bb´, cc´= armature windings (stator)
FF´= field or exciting winding (rotor)
DD´, QQ´= damping windings (rotor)

Fig. 2. Synchronous machine representation showing the concentrated windings and corresponding axes

Expressions that relate synchronous machine voltages, fluxes and currents are shown in (6) and (7).

$$[v] = -[R][i] - \frac{d[\lambda]}{dt} \quad (6)$$

$$[\lambda] = [L][i] \quad (7)$$

where:
$[v]$, $[i]$, $[\lambda]$ - column matrices of voltages, currents and linkage fluxes for phases “a”, “b”, “c” of the stator, rotor field excitation “F”, and the “D” and “Q” damping winding components, respectively;
$[R]$ - diagonal matrix of resistances of the windings “a, b, c, F, D, Q”;
$[L]$ - inductance matrix.

The inductance matrix $[L]$ is formed as follow:

- Main diagonal elements:
For i = a, b, c (stator self-inductances)

$$L_{ii} = L_S + L_M \cos[2(\theta + \alpha_{ii})] + \ell_i \quad (8)$$

For i = F, D, Q (rotor self-inductances)

$$L_{ii} = L_i + \ell_i \quad (9)$$

- Other matrix elements:
For i or j = a, b, c and i ≠ j (stator mutual-inductances)

$$L_{ij} = -M_S - L_M \cos[2(\theta + \alpha_{ij})] \quad (10)$$

For i = a, b, c and j = F, D (mutual inductances between stator and rotor, direct axis)

$$L_{ij} = M_j \cos(\theta + \alpha_{ij}) \tag{11}$$

For i = a, b, c and j = Q (mutual inductances between stator and rotor, quadrature axis)

$$L_{ij} = M_j \sin(\theta + \alpha_{ij}) \tag{12}$$

For i or j = F, D, Q and i ≠ j (rotor mutual-inductances)

$$L_{ij} = M_{ij} \cos\alpha_{ij} \tag{13}$$

where:

θ - displacement angle between the axes of the stator phase "a" and the rotor "F";

L_S, L_M - constant parts of a stator phase self-inductance;

L_i - constant parts of rotor self-inductance and of direct and in quadrature damping winding axis: i = F, D, Q;

ℓ_i - leakage inductance of winding i;

M_S - constant part of the mutual inductance between stator phases;

M_j - constant parts of the mutual inductance between a given stator phase and the windings "F", "D" and "Q".

The values of α_{ij} are:

$\alpha_{aa}=0$, $\alpha_{bb}=-2\pi/3$, $\alpha_{cc}=2\pi/3$, $\alpha_{ab}=\pi/6$, $\alpha_{ac}=5\pi/6$, $\alpha_{bc}=-\pi/2$, $\alpha_{aF}=0$, $\alpha_{bF}=-2\pi/3$, $\alpha_{cF}=2\pi/3$, $\alpha_{aD}=0$, $\alpha_{bD}=-2\pi/3$, $\alpha_{cD}=2\pi/3$, $\alpha_{aQ}=0$, $\alpha_{bQ}=-2\pi/3$, $\alpha_{cQ}=2\pi/3$, $\alpha_{FD}=0$, $\alpha_{FQ}=\pi/2$, $\alpha_{DQ}=\pi/2$.

The electromagnetic torque is given by (14):

$$T = \frac{p}{2}\sum_i \sum_j i_i i_j \frac{dL_{ij}}{d\theta} \tag{14}$$

where i_i and i_j are the currents in windings i and j, respectively, and the subscripts i or j can represent "a", "b", "c", "F", "D" or "Q" with i ≠ j, and p is the number of poles.

Equation (15) shows the synchronous machine swing expression.

$$J\frac{d^2\theta}{dt^2} = T_T - T \tag{15}$$

where:

T_T - prime mover (wind turbine) torque;

T - electromagnetic torque;

J - inertia moment.

D. Frequency Converter and Control Loop Representations

The frequency converter employed consists of two non-controlled series-connected rectifier bridge and a sinusoidal PWM (Pulse Width Modulation) inverter. In this situation the converter unit behaves like an asynchronous AC-DC-AC link shown in Fig. 3, uncoupling the wind conversion system and the ac electric grid [8].

The inverter makes possible the control of active and reactive powers delivered to/consumed from the system through the proper closed-loop control presented in Fig. 4. The strategy for the control is based on the vector theory [9], which enables the maximum extraction of the available wind energy and also the control of the voltage at the Point of Common Coupling (PCC). The bus voltage control is established by the reactive power supplied to or absorbed from the AC system [10].

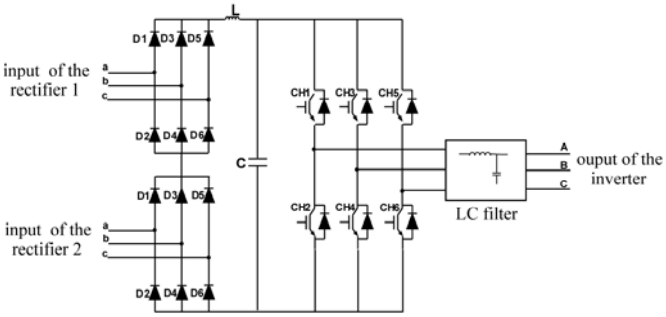

Fig. 3. Frequency converter representation

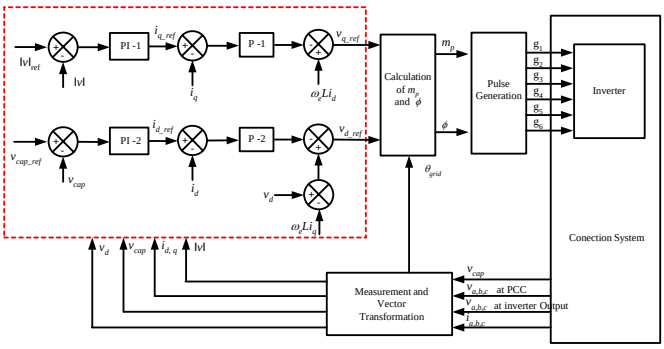

Fig. 4. Inverter control block diagram

From the superior loop it is noticed that, once the voltage module $|v|$ is obtained at the electric grid connection point, this is then compared with a given reference value. The error signal resulted from such comparison is taken to the PI-1 controller, which defines the reference quadrature current, i_{q_ref}. This value is compared with the quadrature current obtained from the vector transformation. Then, the difference is used as the input data for the P-1 proportional controller whose output is compared with the signal generated to eliminate the direct axis coupling in order to produce the reference quadrature voltage, v_{q_ref}.

For the second control loop it is adopted a similar methodology. This time, the input data are the voltage from the dc link and the corresponding reference value supplied. As the output of this loop, it is obtained the reference direct axis voltage v_{d_ref}.

The obtained reference voltages v_{q_ref} and v_{d_ref} are used to determine, through equations (16) and (17), the values of the modulation index, m_p, and the displacement angle, θ, respectively. The index m_p defines the reference voltage magnitude of the PWM control used to adjust the reactive power flow. On the other hand, the angle θ defines the phase shift between the inverter output voltage, e, and the PCC voltage, v, which is used to adjust the active power flow injected into the ac system. It is pointed out that the PWM control requires the reference voltage to be synchronized to the grid voltage. Therefore, the displacement of the network voltage, θ_{grid}, should be taken into account. Such angle is obtained through the process of acquisition of PCC voltages. The angle, ϕ, really used in the control is given by (17).

$$m_p = \frac{\sqrt{v_{d\_ref}^2 + v_{q\_ref}^2}}{v_{cap}} \quad (16)$$

$$\phi = \theta + \theta_{grid} = arc\ tg\left(\frac{v_{q\_ref}}{v_{d\_ref}}\right) + \theta_{grid} \quad (17)$$

E. Transformer Representation

This section aims to present the mathematical modeling for power transformers which is responsible for making compatible the voltage levels of the wind system and electric grid.

Thus, basing on the traditional equivalent circuit and taking into account the non-linear characteristic of the ferromagnetic material of the transformer core, this device can be represented by the equivalent circuit shown in fig. 5 [11].

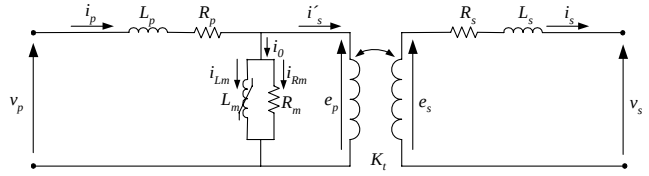

Fig. 5. Transformer equivalent circuit

F. Utility Power Grid Representation

Aiming to model the AC three-phase utility power grid to which the wind system is connected, a simplified model is proposed. The strategy is based on the knowledge of the short circuit level at the PCC (Point of Common Coupling) represented by an impedance (resistance R_{SC} in series with and inductance L_{SC}) and an ideal voltage source (infinite busbar - *e*). The three-phase utility model allows independent representation of phases "a, b, c" including unbalances and wave form distortions. The representative mathematical expression of the "utility" at PCC is given by (18).

$$[v] = [e] - [R_{SC}][i] - [L_{SC}]\frac{d[i]}{dt} \quad (18)$$

III. COMPUTATIONAL STUDIES

The different units composing the WECS were implemented into a time domain simulator. In order to verify the performance of the proposed system, several simulations were accomplished which consisted in applying a wind signal to the complete system represented by the wind installation and the power grid. Then, it is observed the behaviour of some variables such as: power coefficient, generator speed, voltages and currents. Similar observations can be made for the load connected at PCC in terms of the demanded active and reactive powers.

The following studies refer to the physical arrangement of the WECS given in Fig. 1. The principal wind system parameters, used for the computational simulations in consonance with Fig. 1, are presented in Table I.

TABLE I
DATA OF WECS SIMULATED

Wind Rotor	**Nº of blades**	**Radius [m]**	**Control**	**Axis type**
	3	21	pitch	horizontal
Electric Generator	**f_r [Hz]**	**p [poles]**	**V_r [V]**	**S_r [kVA]**
	17	60	400	600
Converter	**$f_{switching}$ [kHz]**	**C_{dc} [mF]**	**V_{in} [V]**	
	5.0	800	1200	
	L_{dc} [mH]	**Control**	**V_{out} [V]**	
	0.2	PWM	400	
Transformer	**R [%]**	**S_r [kVA]**	**V_{pri} [V]**	
	0.5	1000	400	
	X [%]	**f_r [Hz]**	**V_{sec} [kV]**	
	5	60	13.8	
Utility	**S_{SC} [MVA]**	**V_r [kV]**	**f_r [Hz]**	
	10	13.8	60	
Load	**P [kW]**	**Q [kVAr]**	**V_r [kV]**	**f_r [Hz]**
	650	50	13.8	60

Note: Subscript "r" means "rated" value

Figure 6 illustrates the wind signal used in this work. Besides the base wind speed component (8 m/s), it also contains two gust-type turbulences, beginning, respectively, at 6 and 11 seconds. It is pointed out that the wind signal also includes a component defined as noise, which is responsible for random characteristic of wind. The components of the wind signal have the purpose of verifying the system behaviour under those operative conditions.

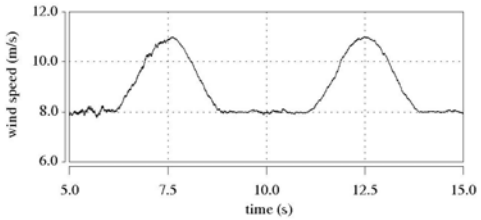

Fig. 6. Incident wind signal applied to the turbine rotor

Figure 7 exhibits the behaviour of the power coefficient (C_p) as established by (4). This figure evidences, as it was expected, the dependence of C_p on wind variations, which is kept around an average value of 0.4 in order to achieve maximum wind-energy efficiency.

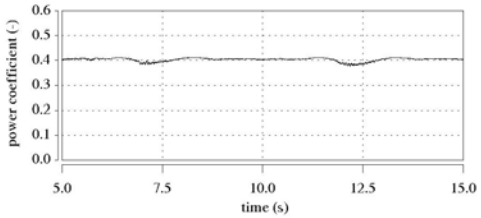

Fig. 7. Power coefficient of wind conversion system

The mechanical speed behaviour of the multipole generator (60 poles) can be observed in Fig. 8. Notice the speed vary from 3.2 (steady-state value) to 3.8 rad/s (peak value), corresponding to voltage and current supply frequencies between 15.3 to 18.2 Hz.

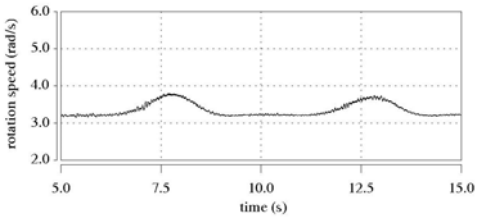

Fig. 8. Synchronous generator Mechanical speed

Figure 9 exhibits the three-phase voltages at synchronous generator terminals which follow the generator speed behaviour, caused by the wind signal applied. Fig. 10 shows the zoom of the voltages given in Fig. 9. It can be clearly seen that they are non-sinusoidal, but with a low harmonic content where the individual harmonics are related to the traditional twelve-pulse rectifier operation.

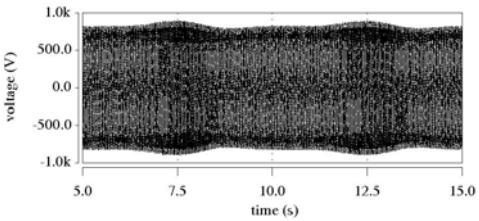

Fig. 9. Phase-to-phase synchronous generator voltages

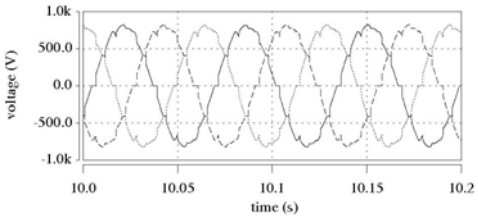

Fig. 10. Zoom of the phase-to-phase synchronous generator voltages of Fig. 9

Current waveforms corresponding to the voltages shown in Figs. 9 and 10 are depicted in Figs. 11 and 12, respectively. The latter illustrates in detail the current waveforms that are in agreement with those observed in a non-controlled rectifier bridge, also with a low harmonic content (characteristic harmonics). Again the current waveform shows a typical behaviour of a twelve-pulse rectifier.

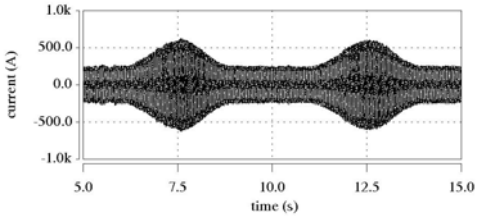

Fig. 11. Synchronous generator three-phase currents

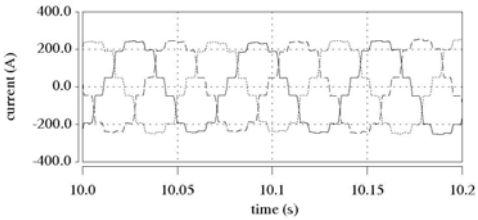

Fig. 12. Zoom of the synchronous generator currents of Fig. 11

Complementary, Figs. 13 and 15 exhibit, respectively, the voltage and current waveforms at PCC. Fig. 14 shows the zoom of the voltages given in Fig. 13. The current waveform distortions observed in Fig. 16, are due to the inverter control strategy (PWM) used in the conversion system AC-DC-AC. As known, this provokes harmonic orders in the switching frequency band (5 kHz). In comparison to other solution using electronic conversion the level of THD appears to be quite reasonable [12], and it is in accordance with measured values in real systems [13], [14].

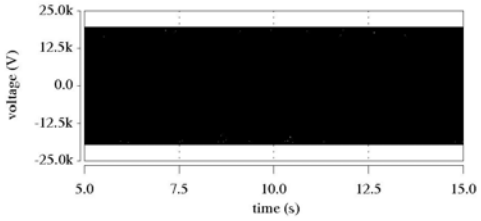

Fig. 13. Three-phase voltages at PCC

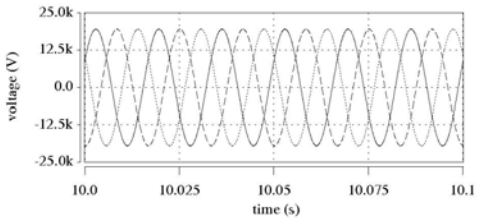

Fig. 14. Zoom of the three-phase voltages at PCC

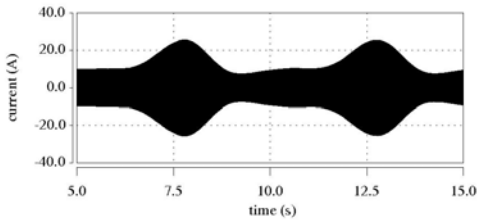

Fig. 15. Three-phase currents at PCC

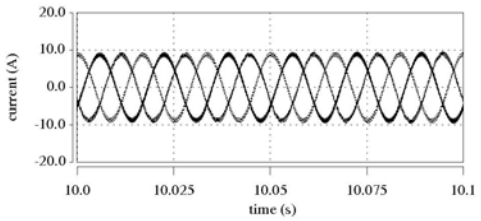

Fig. 16. Zoom of the three-phase currents at PCC

Figure 17 presents the capacitor voltage at the dc link. Before the gust occurrences, it is observed that the voltage value is around 1 pu. Once the event is initiated, due to the larger availability of energy, the voltage increases, reaching a value close to 1.03 pu, and, at the end of the gust, this falls to 0.96 pu.

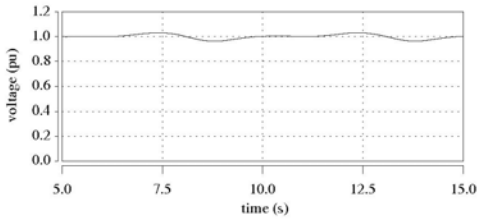

Fig. 17. Capacitor voltage at the converter dc link

During the gust, the control acts so as to provide a larger active power, as verified in Fig. 18. After reaching the maximum value, the power is decreasing. In consequence of the increase of the active power supplied by the WECS, a gradual discharge of the capacitor is found. Then, the active power supply also shows a corresponding behavior. The capacitor is then recharged and so on.

A similar relationship to that described for the dc link voltage and the active power is verified between the PCC voltage and the reactive power, as shown in Fig. 16. The reactive power generated by the wind system starts to supply a slightly large amount of reactive power in response for the voltage oscillation at the PCC. This performance aims the reestablishment of the voltage level. Once the turbulence ceases, the system goes towards the pre-disturbance condition.

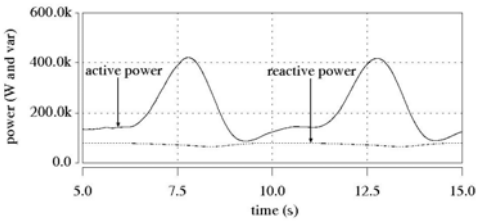

Fig. 18. Active and reactive powers supplied by WECS

IV. CONCLUSION

This paper is concerned with the time domain representation of Wind Energy Conversion System (WECS) components, using synchronous generators connected to the utility grid through frequency converters. The models were implemented in a computational package allowing ideal and non-ideal transient and steady-state operation studies. The developed program can be used for WECS design and component specification as well as to investigate the overall WECS and ac grid operation.

Studies were performed to highlight the program applicability under ordinary operation conditions. The results showed several important variables throughout the WECS system, beginning with wind speed and going up to the ac grid voltage behavior (PCC). It can be concluded from the results that the WECS model implemented has provided performance results in good agreement with expected behavior of commercial wind energy conversion installations. Other situations such as non ideal and more critical operation conditions could also be easily handled with the developed software.

It is recognized that the software is to be further investigated and by comparing computational results to corresponding ones derived from real wind systems, it will possible to validate the overall methodology and program. So far, only the PCC information was available and both the software performance and the measurements were shown to be in good agreement.

ACKNOWLEDGEMENT

The authors acknowledge the financial support received from Brazilian Council CNPq for the doctorate scholarship and from Furnas Power Utility for the accomplishment of a P&D project, which resulted in this paper.

REFERENCES

[1] L. Gertmar, “Power Electronics and Wind Power”, *Dep. of Industrial Electrical Engineering and Automation*, LTH/IEA, Lund University, Sweden, EPE Toulouse, 2003.

[2] S. Heier, “Grid Integration of Wind Energy Conversion Systems”, *John Wiley & Sons, England*, 1998.

[3] J. G. Slootweg, S. W. H. de Hann, H. Polinder and W. L. Kling, “General Model for Representing Variable Speed Wind Turbines in Power System Dynamics Simulations”, *IEEE Transactions on Power Systems*, Vol. 18, N°. 1, pp. 144 – 151, February, 2003.

[4] V. Akmatov, H. Knudsen and A. H. Nielsen, “Advanced Simulation of Windmills in the Electric Power Supply”, *Electric Power Energy Systems*, Vol. 22, n. 6, pp. 421 – 434, July, 2000.

[5] Agência Nacional de Energia Elétrica (ANEEL), *Atlas de Energia Elétrica do Brasil*, available: www.aneel.gov.br

[6] P. M. Anderson and A. Bose, “Stability Simulation of Wind Turbine Systems”, I*EEE Transactions on Power Apparatus and Systems*, Vol. PAS 102, N° 12, pp. 3791 – 3795, December,1983.

[7] P.Kundur, “Power System Stability and Control”, *McGraw-Hill*, Inc, 1994.

[8] R. M. Hilloowala and A. M. Sharaf, “A Utility Interactive Wind Energy Conversion Scheme with an Asynchronous DC Link Using a Supplementary Control Loop”, *IEEE Transactions on Energy Conversion*, Vol. 9, N°. 3, September, pp. 558 – 563.

[9] C. Schauder, H. Mehta, “Vector Analysis and Control of Advanced Static Var Compensators”, *IEE Proceedings-C*, Vol. 40, N°. 4, pp. 299 – 306, July, 1994.

[10] Z. Chen and E. Spooner, “Grid Power Quality with Variable Speed Wind Turbines”, I*EEE Transactions on Energy Conversion*, Vol. 16, N°. 2, pp. 148 – 154, June, 2001.

[11] G. Allan, “Electrical Transients in Power Systems”, *John Willey*, 1971.

[12] D. Schulz, R. E. Hanitsch and C. Saniter, “Causes of Harmonics and Interharmonics in Wind Energy Converters”, *RIO 5 - World Climate & Energy Event*, Rio de Janeiro, Brazil, pp. 169-170, February, 2005.

[13] D. Schulz, R. E. Hanitsch, K. Moutawakkil and C. Saniter, “Power Quality Behaviour of Large Parks with variable Speed Wind Energy Converter”, *17th CIRED - International Conference on Electricity Distribution*, Barcelona, Espanha, Session 4, Paper No 28, pp. 1-4, May, 2003.

[14] D. Schulz and R. E. Hanitsch, “Power Quality Investigations of Different 1.5 MW Wind Energy Converter”, *Proceedings 37th Universities Power Engineering Conference*, Stafford, UK, 2002.